

Magnetization damping in polycrystalline Co ultra-thin films: Evidence for non-local effects

J-M. L. Beaujour, J. H. Lee, A. D. Kent

Department of Physics, New York University,

4 Washington Place, New York, NY 10003, USA

K. Krycka and C-C. Kao

Brookhaven National Laboratory, Upton, New York 11973, USA

(Dated: October 2, 2018)

Abstract

The magnetic properties and magnetization dynamics of polycrystalline ultra-thin Co layers were investigated using a broadband ferromagnetic resonance (FMR) technique at room temperature. A variable thickness ($1 \text{ nm} \leq t \leq 10 \text{ nm}$) Co layer is sandwiched between 10 nm thick Cu layers (10 nm Cu| t Co|10 nm Cu), while materials in contact with the Cu outer interfaces are varied to determine their influence on the magnetization damping. The resonance field and the linewidth were studied for in-plane magnetic fields in field swept experiments at a fixed frequency, from 4 to 25 GHz. The Co layers have a lower magnetization density than the bulk, and an interface contribution to the magnetic anisotropy normal to the film plane. The Gilbert damping, as determined from the frequency dependence of the linewidth, increases with decreasing Co layer thickness for films with outer Pt layers. This enhancement is not observed in structures without Pt layers. The result can be understood in terms of a non-local contribution to the damping due to spin pumping from Co through the Cu layer and spin relaxation in Pt layers. Pt layers just 1.5 nm thick are found to be sufficient to enhance the damping and thus act as efficient “spin-sinks.” In structures with Pt outer layers, this non-local contribution to the damping becomes predominant when the Co layer is thinner than 4 nm.

PACS numbers:

I. INTRODUCTION

The magnetization dynamics of ultra-thin magnetic layers (<10 nm) is of great scientific and technological interest, as such layers are widely used in spin-injection and transport studies as well as in magnetic devices. There has been particular interest in non-local effects whereby layers separated from a magnetic layer influence its magnetization dynamics through non-magnetic (NM) metallic contact layers, i.e., via conduction electrons. Such effects were modeled and studied in the early 1970's by Silsbee *et al.* [1]. More recently, a scattering theory approach has been employed to describe the enhancement of the damping [2, 3]. There have also been experiments [4, 5, 6] which indicate quantitative agreement with this theory based on interface parameters that can be determined from *ab-initio* calculations [7] as well as transport experiments [8].

The current interest in this mechanism is at least threefold. First, it is a fundamental mechanism of damping that can provide important information on interface and bulk spin diffusion. Second, the effect is known to play an important role in current-induced magnetization excitations in spin-transfer devices [9]. In such devices, a few nanometer thick magnetic layer is embedded between NM layers which separate it from a thick ferromagnetic layer that sets the spin-polarization of the current [10]. The threshold current density for magnetic excitations is proportional to the damping [11]. In order to understand the physics of spin transfer, it is therefore important to investigate the effect of adjacent NM layers on the magnetic relaxation of ultra-thin films. Finally, from a technological point of view, this process provides a way to engineer the damping, which is important for high speed magneto-electronic devices.

Mizukami *et al.* studied the Gilbert damping of sputtered NM| t Py|NM films as a function of the FM layer thickness ($2 \leq t \leq 10$ nm) and for different adjacent non-magnetic metals NM=Cu, Pd and Pt using a X-band FMR technique [4]. The damping was found to be consistent with the spin pumping picture: increasing with decreasing Py thickness for the films with NM=Pt and Pd only. Further, the magnetization damping of Cu|Py| L Cu|Pt structures as a function of Cu layer thickness L and with fixed Py thickness, showed evidence for a non-local effect. However, the non-local damping has been studied mainly in NM| t FM|NM structures as a function of the FM layer thickness and varying the material directly in contact with the FM layer [4, 6]. There have also been no experimental studies of

polycrystalline Co layers, which are widely used in spin-transfer devices.

In this paper, we report systematic studies of the thickness dependence of the linewidth and Gilbert damping of ultra-thin Co layers in $||y_1 \text{ Pt}| \text{Cu}| t \text{ Co}| \text{Cu}| y_2 \text{ Pt}||$ structures. The thickness of the Cu layers in contact with Co is kept fixed at 10 nm, which is chosen to be less than the spin-diffusion length in Cu. The Pt layers have no direct interface with the FM layer. The structure is modified by removing one or both of the Pt layers (y_1 or $y_2 = 0$). The observation of changes in the Gilbert damping confirm the non-local nature of this damping mechanism and the data allow for quantitative analysis of the interface spin-mixing conductances in the scattering theory approach.

The paper is organized as follows. In section II, the film fabrication and the FMR setup are described. Section III explains the method of analysis of the resonance field and linewidth. In section IV, the resonance field and the effective demagnetization field are studied as a function of Co layer thickness. The FMR linewidth and the Gilbert damping data are presented. This is followed by a discussion of the dependence of the Gilbert damping on the Co layer thickness for films with and without Pt and a quantitative analysis of the data.

II. EXPERIMENTAL TECHNIQUE

Four series of films were fabricated with the layer structure $||y_1 \text{ Pt}| 10 \text{ nm Cu}| t \text{ Co}| 10 \text{ nm Cu}| y_2 \text{ Pt}||$ on GaAs substrates. First, symmetric structures with a variable thickness of Co between Pt and Cu layers were grown with $y_1 = y_2 = 1.5 \text{ nm}$ and $1 \leq t \leq 10 \text{ nm}$. The second set of samples were asymmetric, without the top Pt layer ($y_1 = 1.5 \text{ nm}$ and $y_2 = 0$), and with Co of 1.5, 2 and 2.5 nm thickness. In addition, films without Pt layers ($y_1 = y_2 = 0$), with Co of 2 and 3 nm thickness were fabricated. In the fourth and final set of films, the thickness of the Pt layers was varied from 0 to 5 nm in a symmetric way with $y_1 = y_2 = 0, 1.5, 3$ and 5 nm with a fixed Co layer thickness of $t = 2 \text{ nm}$. Note that the studies in which Pt layer thicknesses were varied focused on thin Co layers because the non-local effect on the damping were found to be significant only in Co layers thinner than 4 nm.

Films were prepared by a combination of electron-beam (Co, Pt) and thermal (Cu) evaporation in an UHV system at a base pressure of 5×10^{-8} Torr on polished semi-insulating

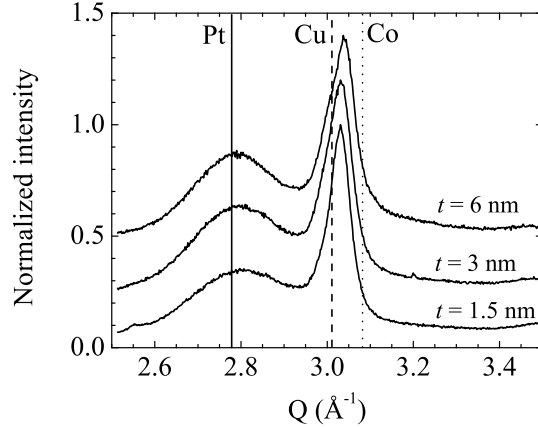


FIG. 1: X-ray data of $||\text{Pt}|\text{Cu}|t \text{ Co}|\text{Cu}|\text{Pt}||$ films with $t = 1.5, 3$ and 6 nm. The curves for the films with 3 and 6 nm Co layer were shifted up for clarity. The vertical solid, dashed and dotted lines show the Q for nominal fcc Pt, Cu and Co respectively.

$4 \times 6 \text{ mm}^2$ GaAs wafers. Note that the chamber is equipped of an in-situ wedge growth mechanism that enables the fabrication of a number of samples with different Co or Pt thickness in the same deposition run, without breaking vacuum. The evaporation rate for Co and Cu were 0.5 and $0.8 \text{ \AA}/\text{sec}$ respectively.

X-ray measurements were conducted on $||\text{Pt}|\text{Cu}|t \text{ Co}|\text{Cu}|\text{Pt}||$ with $t = 1.5, 3$ and 6 nm (Fig. 1). The reflectivity scans were taken at 19 keV using a Bicon point detector. The intensity was first normalized by a beam-monitoring ion chamber, and then each scan was rescaled to reach a maximum of one. The films are polycrystalline and Pt, Cu and Co have an fcc structure with (111) as the crystallographic growth direction. Note that the peak at $Q \sim 3 \text{ \AA}^{-1}$ shifts slightly between the (111) nominal values for Co and Cu depending on how much Co is present. An undistorted bcc (the most intense peak of 110 for Co would be at 3.15 \AA^{-1}) is clearly not present, but a distorted bcc with a lattice of 2.8 \AA cannot be ruled out. Note that the peak of intensity at $Q \approx 2.79 \text{ \AA}^{-1}$ from the Pt layer is strong evidence against interdiffusion at the Pt|Cu interface.

The surface topography of the films $||\text{Pt}|\text{Cu}|\text{Co}|\text{Cu}||$ and $||\text{Cu}|\text{Co}|\text{Cu}||$ were studied using non-contact Atomic Force Microscopy (AFM) (Fig. 2). From the analysis of the AFM images, a rms roughness of $\sigma = 1.4 \pm 0.1 \text{ nm}$ was found for films with Pt underlayer and $\sigma = 1.3 \pm 0.2 \text{ nm}$ for films without Pt. The lateral correlation length were $\xi = 19.6 \pm 1.7$

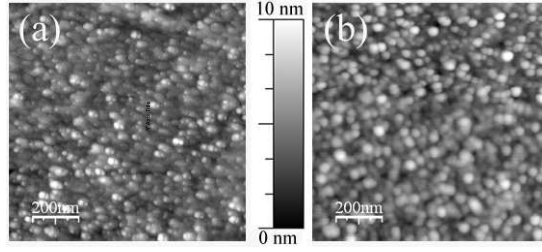


FIG. 2: Grey scale images of AFM scans performed on $1 \mu m^2$ areas of a magnetic film (a) ||Cu|Co|Cu|| and (b) ||Pt|Cu|Co|Cu|| with a Co layer of 2 nm thickness. The rms values of surface roughness is $\sigma = 1.3 \pm 0.2$ nm for (a) and $\sigma = 1.4 \pm 0.1$ nm for (b), and the lateral correlation length is $\xi = 18.0 \pm 0.4$ nm and $\xi = 19.6 \pm 1.7$ nm respectively.

nm and $\xi = 18.0 \pm 0.4$ nm respectively. There is no clear difference in the rms roughness and the correlation length of the film with and without Pt, suggesting that 1.5 nm Pt does not alter the growth of the subsequent Cu|Co|Cu trilayers. The rms roughness is about 6% of the film thickness, which is typical of films prepared by evaporation.

FMR measurements were conducted in an in-plane field geometry at room temperature employing a coplanar waveguide (CPW) as an ac magnetic field generator and inductive sensor [12]. The CPW was fabricated on a $350 \mu m$ thick semi-insulating and polished GaAs wafer from a 200 nm thick Au film patterned using bi-layer photolithographic process. It is characterized by a transmission line of $50 \mu m$ width, a gap to the ground plate of $32 \mu m$ and a length of 4 mm, which is designed to have 50Ω impedance above 4 GHz. The CPW was placed into a brass cavity, with its ends connected directly to the ports of a Network Analyzer. Care was taken to avoid magnetic components in the cavity and in all contacts to the CPW. FMR spectra were measured by placing the magnetic sample metal face down on the CPW and sweeping the external magnetic field at fixed microwave frequency while measuring the S-parameters of the transmission line. Our setup enables measurement of the FMR response of Co layers as thin as 1 nm. Fig. 3a shows the geometry of the measurements. The applied field produced by an electromagnet is directed along the axis of the transmission line and perpendicular to the ac magnetic field generated by the CPW. The applied field was in the film plane, and was monitored with a Hall probe sensor that was calibrated using electron paramagnetic resonance (EPR) on 2,2-diphenyl-1-picrylhydrazyl (dpph), a spin 1/2

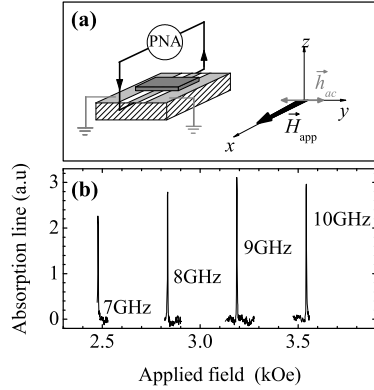


FIG. 3: a) The FMR setup and field geometry. b) Absorption of dpph at different frequencies. The resonance field H_{res} depends linearly on frequency: $H_{\text{res}} = (2\pi\hbar/g\mu_B)f$, and is used to verify the calibration of a Hall sensor used in this study.

system. The measured absorption of dpph is shown in Fig. 3b. The resonance fields were always in agreement with the readings from the Gaussmeter within 10-15 Gauss.

The FMR response was recorded at different frequencies in the range 4-25 GHz. The spectra is measured as the relative change in the transmitted power versus applied field. At 13 GHz for example, the absorption from 5 nm thick Co film at resonance leads to a 0.66% decrease in the transmission. Thus, the susceptibility of the magnetic films only causes a small change in the impedance of the CPW and the absorption line can be analyzed as a small perturbation to the CPW transmission.

III. METHOD OF ANALYSIS OF THE RESONANCE FIELD AND LINEWIDTH

The dynamics of the magnetization can be described in the classical limit by the Landau-Lifshitz equation of motion:

$$\frac{1}{\gamma} \frac{\partial \vec{M}}{\partial t} = \vec{M} \times \vec{H}_{\text{eff}} + \frac{G}{\gamma^2 M_s^2} \vec{M} \times \frac{\partial \vec{M}}{\partial t}, \quad (1)$$

where \vec{H}_{eff} is the effective field, \vec{M} is the magnetization vector and G is the Gilbert damping constant. The gyromagnetic ratio, $\gamma = g\mu_B/\hbar$, is proportional to g , the Landé gyrosopic factor. For a film magnetized in the film plane in an ac field, the resonance condition is [13]:

$$\left(\frac{2\pi f}{\gamma}\right)^2 = H_{\text{res}} (H_{\text{res}} + 4\pi M_{\text{eff}}) , \quad (2)$$

where for a continuous film, the effective demagnetization field is given by:

$$4\pi M_{\text{eff}} = 4\pi M_s + \frac{2K_s}{M_s t} . \quad (3)$$

M_s is the saturation magnetization. The uniaxial anisotropy field $H_s = 2K_s/M_s t$ is characterized by a $1/t$ thickness dependence, where the anisotropy originates from interface and/or strain-magnetoelastic interactions. If K_s , the uniaxial anisotropy constant, is negative, H_s is directed out-of the film plane, corresponding to a perpendicular component to the magnetic anisotropy. Note that by assuming M_s is independent of thickness the uniaxial anisotropy constant, extracted from $4\pi M_{\text{eff}}$ versus t , can be overestimated.

The Gilbert damping is determined by the frequency dependence of the FMR linewidth ΔH [14]:

$$\Delta H(f) = \Delta H_0 + \frac{4\pi G}{\gamma^2 M_s} f , \quad (4)$$

where the slope of $\Delta H(f)$ is the intrinsic contribution to the linewidth, and is proportional to the Gilbert damping constant G . ΔH_0 , the zero-frequency intercept, is usually considered to be an extrinsic contribution to the linewidth. ΔH_0 is sensitive to the film quality: the highest quality films typically exhibit a smallest residual or zero field linewidth [14, 15].

IV. RESONANCE FIELD

Fig. 4 presents the normalized FMR peak at 13 GHz for a selection of ||Pt|Cu| t Co |Cu|Pt|| films. The absorption lines were normalized by subtracting the background signal and dividing by the relative change in transmission at resonance. The lineshape of the FMR curves is typically Lorentzian. Note that we observed asymmetric lineshapes at some frequencies, associated with the measurement method. Distortion of the FMR lineshapes originates from the mixing of the absorptive and dispersive components of the susceptibility (see Ref. [16]). Fig. 5 shows the thickness dependence of the resonance field H_{res} at 14 GHz for films with and without 1.5 nm Pt. The resonance field is practically constant ($H_{\text{res}} \approx 1.2$ kOe) when the Co layer thickness is larger than 5 nm. For thinner layers, H_{res} increases with decreasing t , reaching a value of 1.6 kOe for the film with 1 nm Co layer. The films with the same thickness of Co exhibit about the same resonance field, independent of the presence of

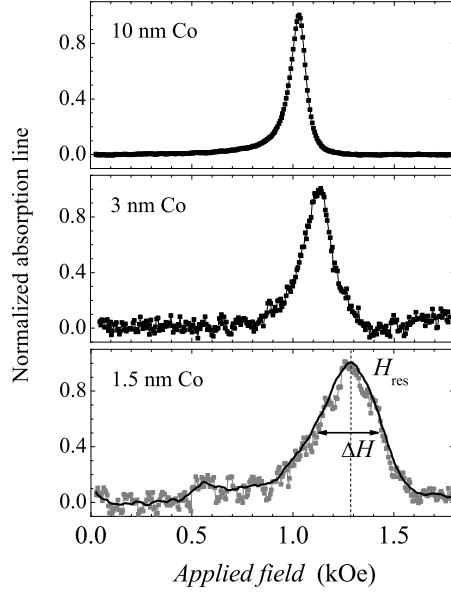


FIG. 4: Typical absorption line at 13 GHz for $||\text{Pt}|\text{Cu}|t \text{ Co}|\text{Cu}|\text{Pt}||$ film with $t = 10, 3$ and 1.5 nm. With decreasing Co thickness the absorption line shifts to higher field and broadens.

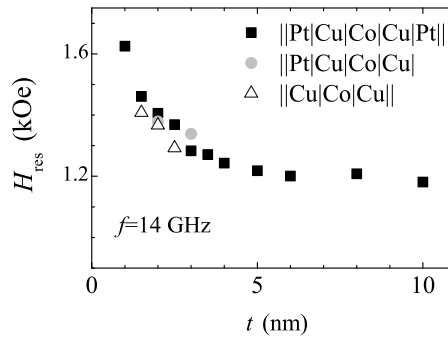


FIG. 5: Thickness dependence of the resonance field at 14 GHz.

the Pt layers. The run-to-run variations in magnetic properties from small changes in film deposition conditions, for instance, are significantly less than the changes in H_{res} observed in the very thin film limit.

The resonance field was measured at different frequencies (Fig. 6). The effective demagnetization, $4\pi M_{\text{eff}}$, and the g-factor were found by fitting f^2/H_{res} vs. H_{res} to Eq. 2. The slope of f^2/H_{res} gives the g-factor and the zero frequency intercept provides the effective

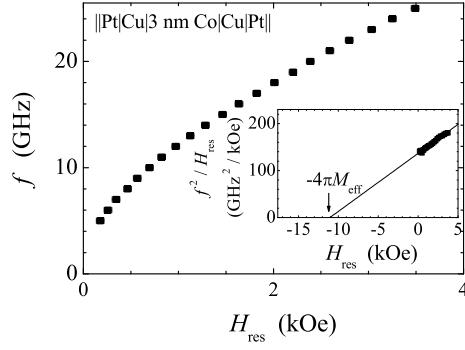


FIG. 6: The frequency dependence of the resonance field for a $||\text{Pt}|\text{Cu}|t\ 3\ \text{nm}\ \text{Co}\ |\text{Cu}|\text{Pt}||$ film. The inset shows f^2/H_{res} vs. H_{res} .

demagnetization field (see the inset of Fig. 6). Films with equal Co layer thickness have nearly the same g and $4\pi M_{\text{eff}}$. This suggests that the Pt underlayer and capping layer do not affect the magnetic properties of the films. The effective field exhibits a clear thickness dependence, decreasing from about 15 kOe to about 8 kOe when the Co thickness varies from 10 nm to 1 nm (Fig. 7). The thickness dependence of the effective field can be understood as originating from the presence of an uniaxial anisotropy field that depends on thickness as $1/t$. The magnetization density is assumed to be independent of the film thickness, as Co and Cu are immiscible. The best fit to Eq. 3 gives a saturation magnetization density of $M_s = 1131\ \text{emu}/\text{cm}^3$ and an uniaxial anisotropy constant $K_s = -0.46\ \text{erg}/\text{cm}^2$. The value of M_s is smaller than the magnetization density of bulk fcc Co ($M_s=1400\ \text{emu}/\text{cm}^3$). The negative sign of K_s reflects a perpendicular component of magnetic anisotropy. As noted earlier, the origin of this perpendicular anisotropy may be a magnetic anisotropy associated with Co|Cu interfaces or magnetoelastic interactions associated with strain in the Co layers, which increases with decreasing Co thickness. The results are in good agreement with magnetometry studies of 150 nm thick epitaxial Co|Cu multilayers grown on GaAs substrates, with Co layer thickness ranging from 0.5 to 4 nm [17]. The authors found an average magnetization density $M_s=1241\ \text{emu}/\text{cm}^3$ and an anisotropy constant $K_s = -0.47\ \text{erg}/\text{cm}^2$. The weighted average value of the Landé g -factor is $g = 2.49 \pm 0.14$ (inset of Fig. 7). This is larger than the value reported in the literature for fcc phase Co ($g=2.15$) [18]. Note that in thin layers there is a larger uncertainty in g making it difficult to determine

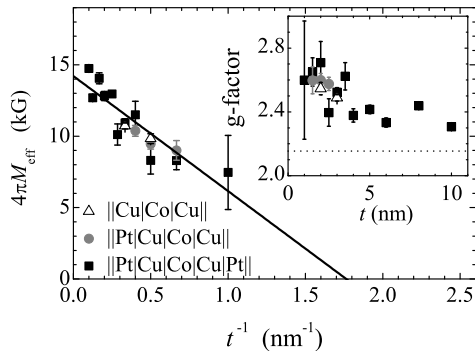


FIG. 7: The effective demagnetization field $4\pi M_{\text{eff}}$ vs. $1/t$. The solid line is the best fit based on Eq. 3. The inset shows the thickness dependence of the Landé g factor. The dashed line gives the value of g for fcc bulk (2.15).

the thickness dependence of the g -factor.

V. LINEWIDTH AND GILBERT DAMPING

The linewidth was studied as a function of frequency and Co layer thickness. As mentioned earlier (section IV), we observed asymmetry in the FMR lineshape at some frequencies. In those cases, the half power linewidth was extracted using the procedure described in Ref. [16]. The linewidth at 10 and 14 GHz is plotted versus the thickness in Fig. 8 for the films with and without Pt. For thick films ($t \geq 5$ nm) with two Pt outer layers, ΔH is practically independent of thickness. However, the linewidth of thinner films ($t < 5$ nm) increases strongly with decreasing Co layer thickness. The three series of films show different increases of the linewidth for thin layers. For instance, the film with 2 nm Co layer thickness and no Pt has a linewidth of 120 Oe at 10 GHz. This is smaller than that of the film with a Pt underlayer ($\Delta H=180$ Oe), and that with two Pt layers ($\Delta H=260$ Oe). The frequency dependence of ΔH enables a determination of the Gilbert damping and the inhomogeneous contribution to the linewidth. Fig. 9 shows the frequency dependence of ΔH for a symmetric film with Pt layers ($y_1 = y_2 = 1.5$ nm) and a 3 nm thick layer of Co. The linewidth depends linearly on frequency, with a zero frequency offset. Below 10 GHz, the data points are more scattered. In this frequency range, the resonance field is of the order of or smaller than the film saturation field, and the absorption line becomes asymmetric. A

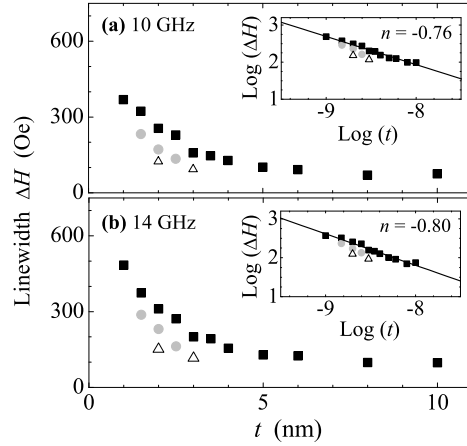


FIG. 8: Thickness dependence of the linewidth at 10 and 14 GHz for the films of series without and with Pt. The insets show the corresponding data on a log-log scale.

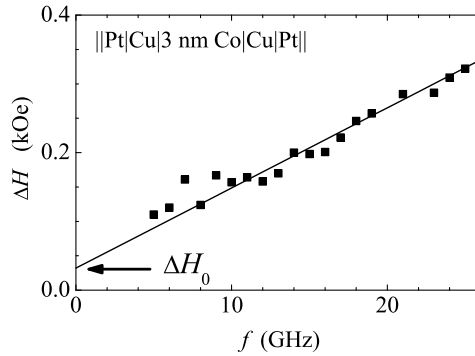


FIG. 9: Typical frequency dependence of the linewidth for the film $||\text{Pt}|\text{Cu}|3 \text{ nm Co}|\text{Cu}|\text{Pt}||$ with Co layer thickness of 3 nm. ΔH_0 and $d\Delta H/df$ are extracted from the linear best fit (solid line).

linear fit to the data is shown in Fig. 9. The thickness dependence of the slope $d\Delta H/df$ and intercept ΔH_0 are shown in Fig. 10. The two parameters exhibit similar thickness dependence: decreasing with increasing Co layer thickness. Therefore, both changes in the Gilbert damping and inhomogeneous broadening contribute to the enhanced linewidth for thin layers. ΔH_0 approaches zero for thick Co reflecting the good quality of these layers. The slope is also practically constant when $t \geq 5$ nm, and it is about three times larger for the thinnest films with two Pt layers.

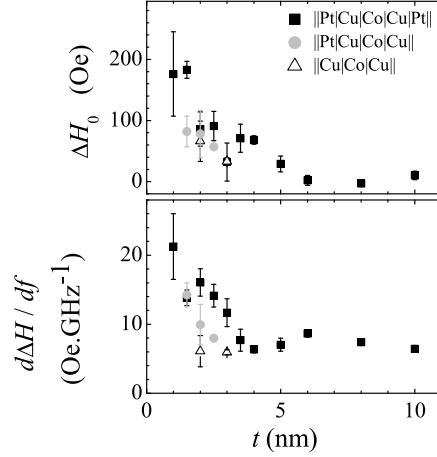


FIG. 10: Thickness dependence of the two contributions to the linewidth: ΔH_0 and $d\Delta H/df$

The Gilbert damping G was estimated from $d\Delta H/df$ (Fig. 10) with Eq. 4. The thickness dependence of the damping is shown in Fig. 11 for the films with and without Pt layers. The damping of $||\text{Cu}|\text{Co}|\text{Cu}||$ films is practically independent of the thickness, and it is about equal to the damping of the films with two Pt layers and thick Co layers ($t > 5$ nm). Note, however, that the inhomogeneous contribution to the linewidth increases with decreasing Co thickness (Fig. 10). The films with one or two Pt layers show an increase in the damping when the Co layer is thinner than 4 nm. 1.5 nm thick Pt layers are thus sufficient to lead to the enhancement of the damping.

In order to investigate whether the damping is a function of the Pt outer layers, films with 2 nm thick Co layers and variable Pt layer thickness were studied. The film structure was $||y \text{ Pt}|\text{Cu}|2 \text{ nm Co}|\text{Cu}|y \text{ Pt}||$. The results are shown in the inset of Fig. 11. The films without Pt have two times smaller damping than the films with Pt. However, remarkably, the damping does not increase further as the Pt layer thickness is increased beyond 1.5 nm. It saturates at a value of about $6 \times 10^8 \text{ s}^{-1}$. This result clearly shows that the main origin of the enhancement of the damping in thin Co layers are the Cu|Pt interfaces. Note that the films of this series, including the ones with $y = 0$ and $y = 1.5$ nm were fabricated a few months after the other series of films. It can be seen that the Gilbert damping of the samples with $y = 0$ and $y = 1.5$ nm, plotted in the inset, are consistent with the films deposited earlier (shown in the main part of Fig. 11).

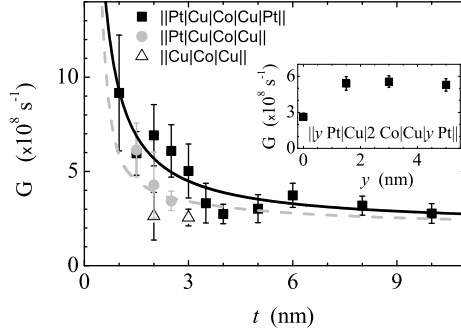


FIG. 11: The magnetic damping versus ferromagnetic layer thickness. The solid line is the best fit of Eq. 5 to $G(t)$ for the films with two Pt layers. The dashed grey line is the calculated thickness dependence of G for the films with a single Pt|Cu interface, and using the parameters found in the earlier fitting. Inset: the magnetic damping versus the thickness of the Pt layers for the films $||y$ Pt|Cu|2 Co|Cu|y Pt|| with 2 nm Co layer.

VI. DISCUSSION AND INTERPRETATION

There are a number of mechanisms which lead to the broadening of FMR linewidth in very thin magnetic films. In the present study, particularly from the effect of “remote” Pt layers on the linewidth, it is clear that non-local interactions are important. We discuss this in detail below and follow this with a brief discussion of two-magnon scattering, which has been extensively discussed in the context of damping in ultra-thin films.

The dependence of G on the thickness of the FM and on the presence of the Pt can be understood in term of spin pumping induced enhancement of the magnetic damping. In this model, the precessing magnetization of the thin Co layer generates a spin current that flows through the Cu layers. In absence of Pt ($||\text{Cu}|\text{Co}|\text{Cu}||$ system), there is not a significant additional damping with decreasing Co layer thickness because the Cu layers are 10 nm thick, which is much thinner than the spin diffusion length in Cu ($\lambda_{\text{sd}} \approx 350$ nm at room temperature [22]). When the Cu layer is adjacent to Pt, a strong spin scatterer, the spin current is absorbed in Pt. There is no back flow of spin current. As a consequence, the Gilbert damping of the FM is enhanced. For a symmetric film with two Pt layers, the effect is more pronounced because the pumping current is absorbed at the two interfaces with Pt. Furthermore, above 1.5 nm Pt, the Gilbert damping does not depend on the thickness of

Pt. In assuming that the film is continuous, a Pt layer as thin as 1.5 nm is thus sufficient to act as a perfect spin sink, i.e., the entire spin current is absorbed. This is in agreement with the results in Ref. [21], where it was reported that the spin loss parameter at the Pt|Cu interface is 0.9 ± 0.1 , which implies about 70% spin randomization at the interface. For very thin Co layers ($t \leq 4$ nm), the non-local damping becomes predominant. It must be mentioned that for the films without Pt capping layer, the top Cu layer, which is in contact with air, might be covered by a native oxide layer. The FMR measurements were conducted within a few days of fabrication of the films. While *a priori* the native oxide layer may affect the damping, our results indicate that this oxide layer must not play a very important role. Indeed, assuming that the oxide layer acts as a spin scatterer, like Pt, it would then be expected that the damping $d\Delta H/df$ of ||Pt|Cu|Co|Cu|| and ||Pt|Cu|Co|Cu|Pt|| with the same Co layer thickness will be equal. Fig. 10 shows that this is not the case.

In a symmetric structure ||NM₂|NM₁|FM|NM₁|NM₂||, where NM₂ is a perfect spin sink and NM₁ thickness is much smaller than the spin diffusion length of the material, the Gilbert damping is [3]:

$$G(t) = G_0 + \left(\frac{g\mu_B}{e}\right)^2 \frac{\tilde{G}_{\text{eff}}^{\uparrow\downarrow} S^{-1}}{t}. \quad (5)$$

G_0 is the residual Gilbert damping (bulk damping), S is the surface area of the sample and $\tilde{G}_{\text{eff}}^{\uparrow\downarrow}$ is the effective spin mixing conductance. $\tilde{G}_{\text{eff}}^{\uparrow\downarrow}$ accounts for the spin mixing conductance at the Co|Cu and Cu|Pt interfaces:

$$\frac{1}{\tilde{G}_{\text{eff}}^{\uparrow\downarrow} S^{-1}} = \frac{1}{\tilde{G}_{\text{Co|Cu}}^{\uparrow\downarrow} S^{-1}} + \frac{1}{G_{\text{Cu}}} + \frac{1}{\tilde{G}_{\text{Cu|Pt}}^{\uparrow\downarrow} S^{-1}}, \quad (6)$$

where $G_{\text{Cu}} = 1/(2L\rho)$ is the conductance per spin of the Cu layer of thickness L and resistivity ρ . Using the literature value of the resistivity for pure Cu, $\rho = 1.7 \times 10^{-8} \Omega\text{m}$, the conductance per spin of 10 nm Cu layer is $G_{\text{Cu}} = 2.94 \times 10^{15} \Omega^{-1}\text{m}^{-2}$. In the films ||Pt|Cu|Co|Cu|Pt|| studied here, the Cu thickness (10 nm) is much smaller than the Cu spin diffusion length. In addition, we found that a 1.5 nm Pt layer is sufficient to saturate the additional Gilbert damping, and therefore is a perfect spin sink. The best fit of the thickness dependence of the magnetic damping gives $\tilde{G}_{\text{eff}}^{\uparrow\downarrow} S^{-1} = (0.34 \pm 0.05) \times 10^{15} \Omega^{-1}\text{m}^{-2}$ and $G_0 = 2.09 \pm 0.44 \text{ s}^{-1}$, using the average value of the g-factor reported in section IV. Note that the conductance per spin of a 10 nm Cu layer is about 10 times larger than the estimated effective spin mixing resistance, meaning that the main contributions to the

resistance in the layered structures originates from that associated with the spin mixing at the Cu|Co and at the Cu|Pt interfaces. After correction of the Sharvin conductance [3], the effective spin mixing conductance is $G_{\text{eff}}^{\uparrow\downarrow}S^{-1} = 0.26 \pm 0.04 \times 10^{15} \Omega^{-1}\text{m}^{-2}$. Using the theoretical values of the mixing conductance for Cu|Co ($0.55 \times 10^{15} \Omega^{-1}\text{m}^{-2}$) and Cu|Pt ($1.36 \times 10^{15} \Omega^{-1}\text{m}^{-2}$) given in [3] and the conductance per spin of Cu as calculated above, the effective spin mixing conductance of the films is predicted to be $0.34 \times 10^{15} \Omega^{-1}\text{m}^{-2}$. The experimental value of the effective spin mixing is about 30% smaller than the calculated value. A similar FMR study was conducted on sputtered films with the same structure. An effective spin mixing conductance $G_{\text{eff}}^{\uparrow\downarrow}S^{-1} = 0.41 \pm 0.05 \times 10^{15} \Omega^{-1}\text{m}^{-2}$ was found. The result implies that the interface spin mixing conductance depends on the film deposition method.

We now briefly discuss FMR line broadening due to two magnon scattering. The scattering of magnons by defects and imperfections at the surface and interface of a thin ferromagnetic film produces modes that are degenerate with the FMR mode ($k=0$) [23], leading to an additional contribution to the linewidth. The mechanism is operative when the magnetization vector lies in the film plane, and it is not operative in the perpendicular geometry. Recently, Arias and Mills developed a theory of the two-magnon scattering contribution to the FMR linewidth in ultra-thin films [24]. The theory was found to successfully explain the frequency dependence of the linewidth of epitaxially grown thin films, with defects of rectangular shape [25, 26]. The AFM images (Fig. 2) show that there is no evidence of anisotropy in the topology of the defects at the surface of the polycrystalline films. In this case, according to [24], the two-magnon contribution is proportional to H_{res}^2 and H_s^2 . As shown in Fig. 9, the linewidth increases linearly with the frequency in the range 4-25 GHz. In plotting the data as ΔH versus H_{res} , the trend is similar to a square root dependence, which does not agree with the expected H_{res}^2 dependence predicted by [24]. Furthermore, the authors calculated that one of the signatures of the linewidth broadening from two-magnon scattering is $\Delta H \propto H_s^2$, where the coefficient of proportionality contains information related to the roughness of the film. As the uniaxial anisotropy H_s scales as $1/t$ (Eq. 3), it is predicted that the linewidth increases as $1/t^2$ for the very thin films. The insets of Fig. 8a and 8b shows the linewidth versus the Co layer thickness in log-log plot at two frequencies, $f = 10$ and $f = 14$ GHz respectively. From the linear best fit, we found that ΔH increases as $1/t^n$ with $n \approx 0.8$. We can conclude that the Arias and Mills model of two-magnon

scattering contribution to the linewidth cannot be used to explain the thickness dependence of ΔH . While, in general a two-magnon contribution to the linewidth may be present, it cannot explain the strong increase of the linewidth for very thin films. This can be seen by comparing the films with two Pt layers and those with only the Pt underlayer. The films grown with a Pt underlayer ($y_1 = 1.5$ nm) and with or without top Pt ($y_2 = 1.5, 0$ nm) are expected to have similar microstructure, since the underlayer structure is identical ($|1.5$ nm Pt|10 nm Cu). As a consequence, in the picture of two-magnon scattering induces linewidth broadening, the linewidth of those films should be the same. However, the thickness dependence of ΔH shows that the films with two Pt layers have a larger linewidth than those with a single Pt layer.

VII. CONCLUSION

We have conducted a FMR study of polycrystalline ultrathin Co films embedded between 10 nm Cu. The outer interfaces of Cu were placed in contact with different environments, by adding Pt layers. We have found that very thin Co layers magnetization relaxation processes depend on the non-local environment. The Co layers exhibit a lower magnetization density compared to the bulk material, and an uniaxial anisotropy field perpendicular to the film plane. The large difference between the g-factor value of the ultra-thin Co layer compared to the bulk fcc Co remains an open question.

The FMR linewidth, studied as a function of the Co layer thickness and of the non-local environment, increases with decreasing Co layer thickness. We have provided evidence that the two-magnon scattering mechanism cannot explain the thickness dependence of the linewidth. The inhomogeneous contribution to ΔH increases with decreasing Co layer thickness, independently of the presence of the Pt layer. However, the Gilbert damping, the intrinsic contribution to the linewidth, was found to be function of the Co layer thickness and depends on the non-local environment. In particular, the Gilbert damping increases significantly with decreasing Co layer thickness only in the presence of a Pt|Cu interface. The thickness dependence of G is consistent with the theory of spin pumping. By changing the outer interface environment of |Cu|Co|Cu| by adding or removing Pt in contact with Cu, we gave unambiguous experimental evidence that the damping enhancement is a non-local mechanism. The non-local damping becomes predominant compared with other relaxation

mechanism when the Co layer is a few nanometer thick ($t \leq 4$ nm).

In summary, the adjacent layers material as well as the non-local environment are critical for understanding the magnetization relaxation in ultra-thin FMs. This important result must be taking into account in the study of spin transfer devices.

We appreciate very stimulating discussions with C. E. Patton and J. Z. Sun. This research is supported by NSF-DMR-0405620 and by ONR N0014-02-1-0995.

-
- [1] R. H. Silsbee, A. Janossy, and P. Monod, Phys. Rev. B **19**, 4382 (1979).
 - [2] Y. Tserkovnyak, A. Brataas, and G. E. W. Bauer, Phys. Rev. Lett. **88**, 117601 (2002); *ibid* Phys. Rev. B **66**, 224403 (2002).
 - [3] Y. Tserkovnyak, A. Brataas, G. E. W. Bauer, and B. I. Halperin, Rev. Mod. Phys. **77**, 1375 (2005).
 - [4] S. Mizukami, Y. Ando, and T. Miyazaki, Jpn. J. Appl. Phys. **40** 580 (2001); Phys. Rev. B **66**, 104413 (2002).
 - [5] B. Heinrich, Y. Tserkovnyak, G. Woltersdorf, A. Brataas, R. Urban, and G. E. W. Bauer, Phys. Rev. Lett. **90**, 187601 (2003).
 - [6] J. Foros, G. Woltersdorf, B. Heinrich, and A. Brataas, J. Appl. Phys. **97**, 10A714 (2005).
 - [7] K. Xia, P. J. Kelly, G. E. W. Bauer, A. Brataas, and I. Turek, Phys. Rev. B **65**, 220401 (2002) and ref. therein.
 - [8] G. E. W. Bauer, Y. Tserkovnyak, D. Huertas-Hernando, and A. Brataas, Phys. Rev. B **67**, 094421 (2003) and ref. therein.
 - [9] J. Z. Sun, J. Appl. Phys. **97**, 10C714 (2005).
 - [10] see for example, J. A. Katine, F. J. Albert, R. A. Buhrman, E. B. Myers, and D. C. Ralph, Phys. Rev. Lett. **84**, 3149 (2000) ; B. Oezylmaz, A. D. Kent, D. Monsma, J. Z. Sun, M. J. Rooks, and R. H. Koch, *ibid* **91**, 067203 (2003).
 - [11] J. Z. Sun, Phys. Rev. B **62**, 570 (2000).
 - [12] W. Barry, I.E.E.E Trans. Micr. Theor. Techn. MTT**34**, 80 (1996).
 - [13] C. Kittel, Introduction to Solid State Physics, 7th Edition, p.505.
 - [14] See, for example, D. L. Mills and S. M. Rezende in *Spin Dynamics in Confined Magnetic Structures II*, edited by B. Hillebrands and K. Ounadjela (Springer, Heidelberg, 2002), pp.

27–58.

- [15] W. Platow, A. N. Anisimov, G. L. Dunifer, M. Farle, and K. Baberschke, *Phys. Rev. B* **58**, 5611 (1998) ; Z. Celinski and B. Heinrich, *J. Appl. Phys.* **70** (10), 5935 (1991).
- [16] S. S. Klarickal, P. Krivosik, M. Wu, C. E. Patton, M. L. Schneider, P. Kabos, T. J. Silva, J. P. Nibarger, *J. Appl. Phys.* **99**, 093909 (2006).
- [17] C. H. Lee, H. He, F. J. Lamelas, W. Vavra, C. Uher, and R. Clarke, *Phys. Rev. B* **42**, R1066 (1990); G. Bochi, O. Song, and R. C. O’Handley, *ibid.* **50**, 2043 (1994).
- [18] U. Wiedwald, M. Spasova, M. Farle, M. Hilgendorff, and M. Giersig, *J. Vac. Sci. Technol.* **A19**, 1773 (2001).
- [19] S. Chikazumi and C. D. Graham, *Physics of Ferromagnetism*, Oxford University Press (1997), p.73.
- [20] J. A. C. Bland, B. Heinrich (Eds.), Vols. I and II. *Ultrathin Magnetic Structures*, (Springer, Berlin 1994).
- [21] H. Kurt, R. Loloee, K. Eid, W. P. Pratt, and J. Bass, *Appl. Phys. Lett.* **81** (25), 4787 (2002).
- [22] F. J. Jedema, A.T. Filip, and B.J. van Wees, *Nature (London)* **410**, 345 (2001).
- [23] M. Sparks, R. Loudon, and C. Kittel, *Phys. Rev.* **122**, 791 (1961); R. C. Fletcher, R. C. LeCraw, and E. G. Spencer, *Phys. Rev.* **117**, 955 (1960) ; C. E. Patton, *J. Appl. Phys.* **39**, 3060 (1968) ; M. J. Hurben, and C. E. Patton, *J. Appl. Phys.* **83**, 4344 (1998).
- [24] R. Arias and D. L. Mills, *Phys. Rev. B* **60**, 7395 (1999).
- [25] R. Urban, B. Heinrich, G. Woltersdorf, K. Ajdari, K. Myrtle, J. F. Cochran, and E. Rozenberg, *Phys. Rev. B* **65**, 020402(R) (2001)
- [26] J. Lindner, K. Lenz, E. Kosubek, K. Baberschke, D. Spoddig, R. Meckenstock, J. Pelzl, Z. Frait, and D. L. Mills, *Phys. rev. B* **68**, 060102(R) (2003).
- [27] J. Pelzl, R. Meckenstock, D. Spoddig, F. Schreiber, J. Pflaum and Z. Frait, *J. Phys.: Condens. Matter* **15**, S451-S463 (2003).
- [28] S. J. Yuan, L. Wang, R. Shan, and S. M. Zhou, *Appl. Phys. A* **79**, 701 (2004).